Cytometry PART A
Journal of Quantitative Cell Science

Spectrally and Spatially Resolved Laser-Induced Photobleaching of Endogenous Flavin Fluorescence in Cardiac Myocytes

Alzbeta Marcek Chorvatova,[1,2*] Jana Kirchnerova,[1] Michal Cagalinec,[1,3] Anton Mateasik,[1] Dusan Chorvat Jr[1]

[1]Department of Biophotonics, International Laser Centre, Ilkovicova 3, 84104, Bratislava, Slovakia

[2]Department of Biophysics, Faculty of Natural Sciences, University of Ss. Cyril and Methodius, J Herdu 1, 91702, Trnava, Slovakia

[3]Department of Cellular Cardiology, Institute of Experimental Endocrinology, Biomedical Research Center, Slovak Academy of Sciences, Dubravska cesta 9, 84505, Bratislava, Slovakia

Received 6 May 2018; Revised 19 July 2018; Accepted 30 July 2018

Grant sponsor: European Commission Horizon H2020, Grant number: 654148; Grant sponsor: the Integrated Initiative of European Laser Infrastructures LASERLAB-EUROPE IV; Grant sponsor: Slovak Academy of Sciences, SASPRO, Grant number: 0063/01/02; Grant sponsor: co-financed by Grant sponsor: EC 7th Framework Programme, Marie Curie Actions, Grant number: 609427; Grant sponsor: COFUND; Grant sponsor: Science grant agency VEGA of Ministry of Education, Science, Research and Sport of Slovak Republic, Grant numbers: 2/0123/18, 2/0169/16

*Correspondence to: Dr. Alzbeta Marcek Chorvatova, International Laser Center, Ilkovicova 3, 84104 Bratislava, Slovakia.
Email: alzbeta.marcekchorvatova@ilc.sk

Published online 21 September 2018 in Wiley Online Library (wileyonlinelibrary.com)

DOI: 10.1002/cyto.a.23591

ISAC International Society for Advancement of Cytometry

Abstract

Naturally occurring endogenous fluorescence of flavins, arising in response to excitation by visible light, offers broad opportunity to investigate mitochondrial metabolic state directly in living cells and tissues, including in clinical settings. However, photobleaching, the loss of the autofluorescence intensity following prolonged exposure to light is an inherent phenomenon occurring during the fluorescence acquisition, which can have a negative impact on the recorded data, particularly in the context of measurement of metabolic modulations in pathophysiological conditions. In the presented study, we present a detailed analysis of endogenous flavins fluorescence photobleaching arising in living cardiac cells during spectrally-resolved confocal imaging. We demonstrate significant nonuniform photobleaching related to different bleaching rates of individual flavin components, resolved by linear spectral unmixing of the recorded signals. Induced photodamage was without effect on the cell morphology, but lead to significant modifications of the cell responsiveness to metabolic modulators and its contractility, suggesting functional metabolic alterations in the recorded cells. These findings point to the necessity of inducing limited photobleaching during metabolic screening in all studies involving visible light excitation and fluorescence acquisition in living cells. © 2018 The Authors Cytometry Part A published by Wiley Periodicals, Inc. on behalf of International Society for Advancement of Cytometry

Key terms

flavin; autofluorescence; photobleaching; cardiac myocytes; confocal imaging; spectral unmixing

AUTOFLUORESCENCE, the naturally occurring endogenous fluorescence arising in response to excitation by light is highly advantageous for noninvasive investigation of mitochondrial metabolic state directly in living cells (1). At the same time, photobleaching is the loss of the autofluorescence intensity following prolonged exposure of cells to light and their inherent phenomenon occurring during the fluorescence acquisition has a negative impact on the recorded data (2). It arises during long periods of detection of the fluorescence and can therefore significantly impact-driven conclusions. As it is also accompanying fluorescence recordings in living biological systems, it can therefore represent an essential limitation of physiological studies, such as metabolic imaging. Indeed, excessive illumination in the ultraviolet range to acquire NADH autofluorescence is associated with mitochondrial fission and swelling (3). Moreover, significant loss in FAD autofluorescence in brain slices was accompanied by changes in tissue pO_2, field potential and $[K^+]_o$ (4). In addition, ultrashort laser pulses in two-photon excitation negatively affected cell vitality and reproduction (5). There is a long effort to avoid phototoxicity in live fluorescent microscopy (6). In this article, our aim was to compare photobleaching in a typical confocal microscopy experiment.

Bulk of the cellular autofluorescence signal, generated after excitation with visible blue/green light, is localized in mitochondria and has its origin in the chemical reactivities of flavins and flavoproteins emitting in a broad spectral range from 490 to 560 nm (7–10). Fluorescence of flavins involved in the mitochondrial energy metabolism is dependent on their redox state (11). Due to this fact, the redox fluorimetry, based on the recording of the fluorescence increase in the oxidized state and its decrease in the reduced state, offers a possibility of investigation of the mitochondrial metabolism and its connection to mitochondrial respiration in isolated mitochondria (12), in living cells (7,8,13), and/or in tissues (4,10,14).

Flavin fluorescence is for long recognized to be subjected to photobleaching both in in vitro (15) and in vivo conditions (13). Despite the fact that autofluorescence signal was known to originate from multiple sources, in previous studies—where the cellular autofluorescence was recorded using bandpass or high pass detection—the photobleaching was only considered to lead to decline in fluorescence maxima (9) and/or to under- or over-estimation of fluorescence changes (13). Since the bandpass detection does not allow recognition of photobleaching characteristics of individual components, such assumptions were based on the premise that photobleaching of all flavin components is uniform. Despite the fact that the photobleaching was acknowledged in multiple spectrally resolved studies (16–20), spectral characteristics of the signal decrease due to photobleaching were not fully assessed. In these cases, the authors only referred to the decrease in the total flavin cellular autofluorescence and focused at the appearance of secondary changes of the cell morphology due to photodamage (21) or introduced a criterion of "normal" responsiveness instead (20). We previously compared photobleaching of individual NAD(P)H fluorescence components using time-resolved fluorescence spectroscopy (22) and showed only little effect. However, to be able to better comprehend the limitations of metabolic imaging, the primary loss of fluorescence during photobleaching and its functional implications needs to be further elucidated.

The aim of this study was to determine whether the photobleaching of flavin fluorescence leads to over- or underestimation of fluorescence intensity only, and/or it also involves altered cell functioning. We approached this issue by applying spectrally resolved confocal laser scanning microscopy on living cardiomyocytes and by subsequent linear unmixing of individual autofluorescence components from the multispectral images (8). In this way, we were able to perform simultaneous detection of individual spectral components of flavin fluorescence involved in various pathways of mitochondrial metabolism and respiration. The loss of autofluorescence due to photobleaching was measured by repetitive confocal laser scanning and imaging of freshly isolated cardiac myocytes. In this study, we evaluated photobleaching using a single photon excitation, as is the case of most microscopy studies, including those employing fluorescent probes. We have examined spectral characteristics and radiant exposure dependency of photobleaching of flavin fluorescence, as well as responsiveness of cells to mitochondrial modulators after photobleaching.

Materials and Methods

Preparation of Cells and Solutions

Animals. The work was performed on adult Wistar rats (weighting 290–350 g, Dobra Voda, Slovakia). All procedures comply with the Ethical Committee of the Pharmaceutical Faculty, Comenius University, Bratislava, Slovak Republic. The investigation conforms to the Guide for the Care and Use of Laboratory Animals published by the US National Institutes of Health (NIH Publication No 85-23, revised 1996).

Isolation of cardiomyocytes and handling during experiment. Left ventricular myocytes were isolated following retrograde perfusion of the heart with proteolytic enzymes (23,24), using 1.0 mg/ml collagenase (type II; Gibco-BRL, Crewe, UK) and 0.1 mg/ml protease (Sigma-Aldrich, Steinheim, Germany) in low $CaCl_2$ (50.0 μl) at 35 ± 1°C. The pellets of myocytes were resuspended in enzyme-free isolation solution containing 0.75 μl $CaCl_2$ (see "Solutions" section for composition) and maintained in a Petri dish at 4°C until use. Only cells that showed clearly defined sarcomere striations and have contracted in a stable way in response to field stimulation were used in this study, in up to 10 h following dissociation.

In each experiment, cells were prefield stimulated at 0.5 Hz for about 3–5 min prior to the recording of images to insure that we work on functional cells with stabilized calcium loading. Pulse generator (Harvard Inst., Digitimer, Hertfortshire, UK) was used for frequency-triggered field-stimulation in a home-made perfusion chamber, equipped with stimulation Pt electrodes. Perfusion at 35 ± 1°C or room (22 ± 1°C) temperature was performed via peristaltic pump at 1 ml/min rate and open surface of perfusion chamber allowed free access to oxygen.

Reagents. Sodium cyanide (NaCN), prepared in water and 2,4-dinitrophenol (DNP) and prepared in DMSO, were used at final concentrations 4.0 μl and 50.0 μl, respectively. KCl, $CaCl_2$, and glucose were purchased from Merck (Darmstadt, Germany), collagenase was obtained from Gibco, and NaCl, $MgCl_2$, and NaH_2PO_4 were obtained from Lachema (Brno, Czech Republic). All other drugs were purchased from Sigma.

Solutions. Isolation solution: The physiological salt solution was used for the isolation and storage of myocytes contained (in μl): NaCl, 130.0; KCl, 5.4; $MgCl_2 \cdot 6H_2O$, 1.4; NaH_2PO_4, 0.4; creatine, 10.0; taurine, 10.0; glucose, 10.0; 4-(2-hydroxyethyl)-1-piperazineethenesulfonic acid (HEPES), 10.0; titrated to pH 7.3 with NaOH. This was supplemented with EGTA or Ca^{2+} at following stages of the isolation procedure, as described previously (23,24).

Basic external solution: Basic external solution perfused on single cardiomyocytes during recording contained (in μl): NaCl, 130.0; KCl, 5.4; $CaCl_2$, 1.8; $MgCl_2$, 1.4; NaH_2PO_4 0.4, glucose, 10.0; HEPES, 10.0; adjusted to pH 7.3 with NaOH or NaCl, 140; KCl, 5.4; $CaCl_2$, 2; $MgCl_2$, 1; glucose, 10; HEPES, 10; pH 7.35 with NaOH.

Instrumentation

Spectrally resolved confocal microscopy. Spectral and spatial distribution of flavin fluorescence was determined using confocal laser scanning microscopy, Zeiss LSM 510 Meta detector fitted on Axiovert 200 (Zeiss, Jena, Germany). Images were collected with C-Apochromat 40×, 1.2 NA water immersion objective. Confocal pinhole was set to 114 μm (1.51 AU) creating 1.4 μm optical slices. Spectroscopic measurements were performed in response to excitation by 458 nm (16.5 μW) Ar:ion laser line and 633 nm He/Ne laser line (Lasos Lasertechnik, Jena, Germany), which were used for focus and transmission mode imaging. We located a cell and focused at a given region briefly using low intensity 633 nm laser light detected in a transmission mode to avoid photobleaching before the actual scanning of the cell autofluorescence in response to 458 nm laser line. Emission was detected with spectral META detector at 16 channels (477–638 nm) quasi-simultaneously. Using this approach, we gathered information from two passes of eight spectral 10.7-nm-wide channels (477–552 and 563–638 nm) detected subsequently for one scan resulting in 16-channel image. All spectra of cardiomyocyte fluorescence were obtained by selecting area in multispectral images using LSM Image Examiner and were corrected for solvent background by subtracting cell-surrounding area signal from the whole-cell area signal. Total fluorescence intensity was calculated as a sum of intensities in all 16 channels.

Photobleaching rate measurement. Photobleaching in this experiment was induced by consecutive scanning of several regions of interest (approx. 20 μm wide stripes, perpendicular to longer cell axis) within single cardiomyocyte cell at 35 ± 1°C. Variable laser power at 458 nm was applied, controlled by modulation of the laser line intensity by acousto-optics tunable filter (AOTF). Each cell was subjected to six-fold consecutive scanning at different regions, each using different laser power. To prevent the generation of artifacts, each region was shifted laterally within the cell along its longer axis. Fluorescence intensity was presented as a % fraction (± SEM) of the initial intensity obtained during the first scan. Fluorescence was measured in 12-bit precision within the range of λ_{em} 477–638 nm.

Contractility measurement. Effect of photobleaching on cardiomyocyte contractility was observed using fast line-scan protocol. For maximum effect we invoked bleaching by 488 nm laser line (197.2 μW power at the sample space). Fluorescence and transmission images were recorded using excitation by 458 nm laser line. Contraction of the cell was induced by field stimulation at 0.5 Hz at room temperature via Pt electrodes (DS-2A stimulator; Digitimer Ltd., Hertfortshire, UK).

Data analysis. Linear unmixing (LSM Image Examiner) was applied on multispectral images using calculated basic spectral components (8) (component 1, component 2, and component 3 with spectral maxima around 500, 530, and 560, respectively, and residues). The result of this algorithm is a spatial distribution of intensity-coded values of weighting coefficients of individual spectral components. Calculated intensity of basic spectral components was determined as a mean value of its weighting coefficient within the whole cell area. Data are shown as mean ± SEM. Comparison between means was made by Student's *t*-test.

Results

Characterization of the Photobleaching Rate

Our first step was to determine the real power of the excitation laser source. The incident power of 458 nm Ar:ion laser was measured at the specimen plane using calibrated photodiode. We plotted the measured laser power (0.14–16.5 μW) as a function of the software adjustment of the laser line intensity using AOTF tunable filter within 1–100% of its transmission range. The laser power proved to be linear with respect to AOTF settings within the whole recorded range (Fig. 1a).

In the subsequent experiment, in order to reduce the variability in the bleaching rates we have scanned several (n = 5) regions of interest within single cells with increasing laser power. In such arrangement we did not expect any motion effects, such as passive diffusion or active translational processes taking into consideration that the flavin fluorescence originates from flavins in mitochondria, as demonstrated by (21), and also confirmed in our cells (7). Each region of interest was scanned subsequently 6 times.

The energy delivered onto the specimen can be approximated as a product of laser power (0.14–16.5 μW), multiplied by pixel dwell time (15.2 μs), multiplied by number of averaging acquisition scans (16), and finally multiplied by number of subsequential scan (0–5). The pixel size (approx. 0.24 μm) was set as to match the diffraction-limited beam profile (0.27 μm diameter of Airy pattern for the given 40x/1.2 water objective and 458 nm laser). In such settings, neither the movement of the laser beam during scanning nor the sampling/physical focus mismatch induced substantial aberrations and the total radiant exposure of each irradiated point of the sample can be estimated as absorbed energy per pixel area. Decrease in the autofluorescence intensity with respect to different radiant exposure values is shown at Figure 1b. The autofluorescence emission intensities are represented here as a percentage of the initial intensity, measured using the same laser power. Such representation of obtained data allowed us to compare the rate of photobleaching among all experimental adjustments and combinations.

Gathered results revealed exponential decrease of the autofluorescence intensity with each subsequent scan, which was similar for all laser power settings used, although at a different scale. Already during the second scan, we have always recorded an abrupt decrease of the autofluorescence. Subsequent scans lead to ongoing, but slower decrease in the fluorescence emission. Interestingly, we have observed that the autofluorescence decrease due to photobleaching depends on the total radiant exposure rather than on the laser power, following a single exponential decay trend. We can summarize

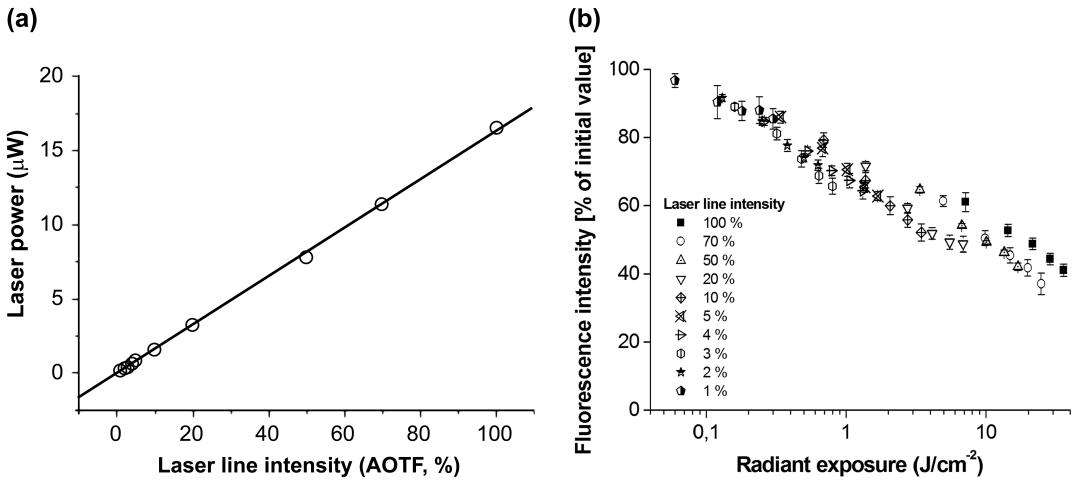

Figure 1. Dependency of autofluorescence photobleaching on radiant exposure. (**a**) Laser power measured at sample space as a function of software adjustment for 458 nm Ar:ion laser line intensity using AOTF. (**b**) Photobleaching of the cell autofluorescence (λ_{exc} 458 nm/λ_{em} 477–638 nm) as a function of radiant exposure using different settings of laser power. Fluorescence intensity is presented as a % fraction (± SEM) of the initial intensity obtained during the first scan.

that the photobleaching rate is proportional to the absorbed energy.

Finally, by modulating the laser power using AOTF, we have tried to find experimental settings for which the photobleaching could be considered negligible. However, despite reducing the photobleaching at lower laser powers, this way of coping with this phenomenon was not successful. The extent of photobleaching remained large even at low excitation powers. For example, consecutive scanning of a small cell area using attenuated laser power to only 1% of the initial laser power resulted in an intensity drop to as much as (at about) 85% of the initial intensity (Figure 1b, insert). In contrast, at excitation levels low enough to prevent photobleaching, the weak fluorescence emission signal resulted in the deterioration of the fluorescence emission spectrum due to poor signal-to-noise ratio.

Spectral Characteristics of Photobleaching

Our second step was to evaluate the effect of consecutive scanning on the spectral characteristics of cardiomyocyte autofluorescence signal. We have collected the autofluorescence from living cardiac cells in response to six successive scanning cycles using 16.5 μW (100%) Ar:ion laser line at 458 nm with 2.56 μs pixel time, performed in a 30 s interval. Cardiomyocyte flavin fluorescence signal was distributed in longitudinal stripes throughout the whole cardiomyocyte area, except for the nuclei (Fig. 2a, upper insert). As we demonstrated previously, this localization corresponds to mitochondria (7). The multiple exposures to excitation by light did not produce any noticeable damage to the cells, as evidenced by no change in the morphological parameters, as well as by absence of hypercontractions, blurred z-lines, and/or osmotic blebs (Fig. 2a, lower insert).

At the same time, the extensive photobleaching of autofluorescence following six successive multispectral scans affected both the total intensity of the emitted light (Fig. 2a), and, more importantly, its spectral shape (Fig. 2b). Using the multispectral detection, it became clear that the photobleaching of autofluorescence, which has a complex spectrum consisting of various fluorescence components (8), is not spectrally homogenous. The marked decrease in the fluorescence after the first scan was caused by photobleaching of molecules emitting predominantly in the blue/green spectral region. Cells scanned for the first time had emission peak at 510 nm. The lowering of the fluorescence was accompanied by a red shift (up to 530 nm) of the emission peak of cells exposed to consecutive scanning, when compared to control conditions. This fact is clearly visible after the normalization of spectra in control conditions and after bleaching.(Fig. 2B). Such comparison of the first and the sixth scans revealed that the bleaching induced clear red spectral shift of about 20 nm.

Differences in Bleaching Rates Among Individual Autofluorescence Components

To further determine the source of spectral heterogeneity observed during photobleaching, we have applied the spectral unmixing algorithm (25) on autofluorescence images (Fig. 3), using the spectra of individual flavin fluorescence components that we have identified previously in these cells (8). The spatial distribution of autofluorescence (Fig. 3a) revealed the spatial heterogeneity in the rate of autofluorescence photobleaching within individual cells. The predominant bleaching of autofluorescence is originating from mitochondria densely distributed in cardiac cells, as opposed to sustained bright autofluorescence originating from lipofuscine granules localized in the perinuclear region. Lipofuscine fluorescence, which presented multiple emission maxima, including the ones in the yellow and the red spectral range, also underwent photobleaching, although at much slower rate (data not shown).

Data gathered at Fig. 3 uncovered differences in the bleaching rates among individual autofluorescence components: the

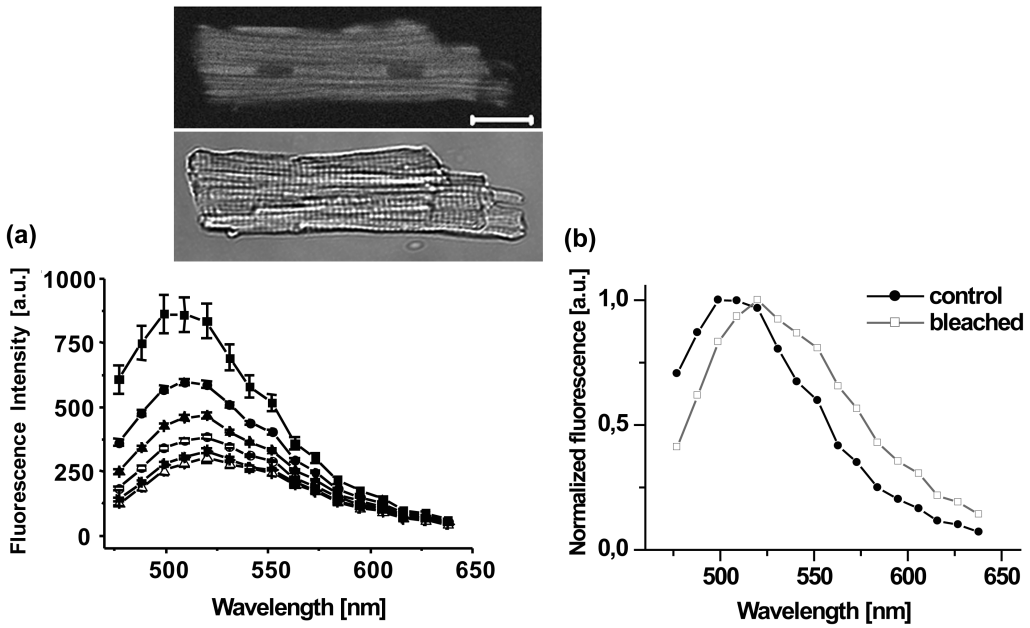

Figure 2. Spectral changes accompanying photobleaching of flavin autofluorescence, induced by consecutive scanning. (**a**) Photobleaching of whole cell autofluorescence (16.5 μW 458 nm laser line, λ_{em} 477–638 nm) during consecutive scanning of autofluorescence. Averaged autofluorescence emission and spectra ± SEM of (n = 5) cells acquired from the multispectral image obtained by first (■), second (●), third(▲), fourth (○), fifth (▶), and sixth (Δ) scan. In the insert, the overall 16 channel (λ_{exc} 458 nm/λ_{em} 477–638 nm) color-coded image of single cardiomyocyte flavin fluorescence obtained by multispectral confocal laser scanning microscopy (upper image) and transmission recording (lower image). Scale bar: 20 μm. (**b**) Comparison of normalized spectrally-resolved flavin fluorescence in control conditions, before bleaching (-●-), and of the fifth scan (-□-). Note the red spectral shift of about 20 nm of the spectrum after bleaching.

spectral component 1, identified in our previous work (8) as corresponding to the flavin bound in electron transfer chain (ETF) and lipoamide dehydrogenase (LipDH), was the most photolabile. This component was clearly responsible for an abrupt fall in the fluorescence intensity after the first scan. The photobleaching rates of the component 2, corresponding to free FAD and of the component 3, corresponding to Acyl-CoA dehydrogenase (8), which are of lower intensity, also presented lower rate of photobleaching. This result explains the red shift of the overall fluorescence, observed after the photobleaching (Fig. 2b). The intensity of the residual channel representing residuals in the fluorescence spectra after unmixing also presented lesser decrease with consecutive scanning.

Responsiveness to Modulation of the Mitochondrial Respiration

In the next step, our goal was to test whether the decrease of autofluorescence caused by photobleaching is reversible and whether it affects the cell responsiveness to metabolic modulation. In these experiments, the whole cell areas were repetitively scanned in 1–5 min intervals and, in the recovery periods between scans, the cells were field stimulated (to induce contractions cell and thus stabilize metabolic loading) and continuously perfused with basic external solution or solutions containing modulators described below, at 35 ± 1°C (Fig. 4a).

In control conditions (without modulators), the initial rapid decrease of fluorescence intensity of precontracted cells had stabilized after the first three scans to about 40% of the original intensity (Fig. 4b, o), as opposed to previous experiments in resting cells, where sixfold consecutive scanning of cells resulted in a drop to about 70% of the initial intensity.

We then analyzed the differences in the responsiveness of the flavin fluorescence intensity to metabolic modulation in the presence (Fig. 4a, i) and in the absence (Fig. 4a, ii) of photobleaching. Modulators of mitochondrial metabolism were applied as previously described (26). We have perfused the cells with solution containing 4 mmol/l NaCN, a well-known blocker of mitochondrial respiration chain at level of Complex IV, and 50 μmol/l 2,4-dinitrophenol (DNP), the uncoupler of mitochondrial respiration and oxidative phosphorylation, already used in our previous work (7,8).

In the first set of these experiments (Fig. 4b, i), we have applied modulators in photobleached cells, after the third consecutive scan. The initial decrease in the total fluorescence intensity was caused solely by photobleaching. Application of 4 mmol/l NaCN leads to clear lowering of the fluorescence after 5 min of exposure (Fig. 4b, i). After switching the perfusion back to basic external solution, the fluorescence intensity returned. However, after 5 min, this rise was only to the level corresponding to the bleached fluorescence intensity, the initial intensity level was not recovered. In contrast, the 50 μmol/l DNP caused significant increase in the fluorescence after 5 min perfusion, but again the 5 min washout of DNP leads to the return to the level of the bleached intensity, not to the initial intensity.

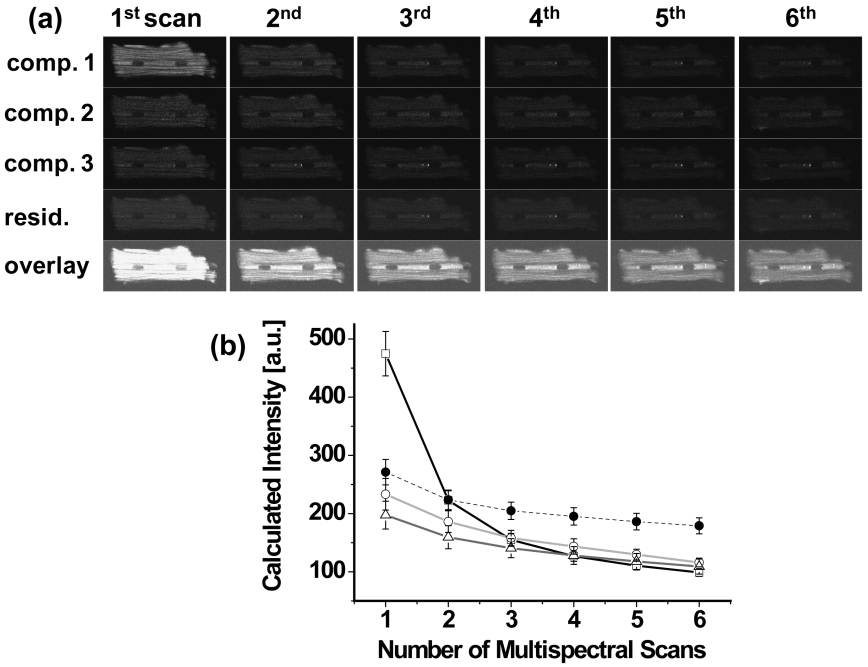

Figure 3. The effect of photobleaching on unmixed individual flavin fluorescence components. (**a**) Representative image of a cardiomyocyte flavin fluorescence resolved by linear unmixing of its spectral components. The individual fluorescence components were resolved from the overall 16 channel (λ_{exc} 458 nm/λ_{em} 477–638 nm) color-coded image of single cardiomyocyte flavin fluorescence (see insert in Fig. 2a). Unmixed images of the autofluorescence components 1–3, including the residues, is shown for six consecutive scans, following photobleaching using 100% (16.5 μW) laser line. (**b**) Comparison of the change in the fluorescence intensity of individual spectral fluorescence component 1 (-□-), component 2 (-●-), component 3 (○), and its residues (Δ) with six consecutive scans computed by principal component analysis. Averaged autofluorescence emission intensity ± SEM (n = 5) is shown.

In the second set of these experiments (Fig. 4b, ii), we have repeated the same experiment in the absence of photobleaching, in order to separate the effect of photobleaching from that of metabolic modulators on cellular autofluorescence. In these experiments, instead of consecutive scanning of the same cell, the autofluorescence emission was collected each time from a different cell in the same batch (Fig. 4b, ii). Similar to the previous experiment, after application of 4 mmol/l NaCN, we have observed a substantial decrease in the fluorescence intensity. After washout of NaCN, the fluorescence returned to the initial intensity. Similarly, substantial increase in the fluorescence intensity after application of 50 μmol/l DNP was followed by a return of the fluorescence intensity to the initial levels following the DNP washout. The response to the application of modulators, namely the DNP, was smaller in cells exposed to multiple scanning (Fig. 4b, i) than in cells exposed to single scanning (Fig. 4b, ii).

We have then compared the spectra of autofluorescence responses to modulators (Fig. 5). The decrease in fluorescence after application of NaCN was observed in the whole flavin part of the autofluorescence spectrum and was comparable in cells without photobleaching (Fig. 5a) and in the photobleached ones (Fig. 5b). The application of DNP was followed by an increase in the fluorescence in both cases predominantly in the green region with maximum at 540 nm. However, in cells scanned for the first time, the autofluorescence increase was much more pronounced than that in cells exposed to multiple scanning, where the autofluorescence increased only slightly. In order to better understand the nature of metabolic change that is taking place in the photobleached conditions, we have evaluated percentage of oxidized nucleotides, as described in our previous work (27). Using conditions in the presence of DNP as the fully oxidized one, and in the presence of NaCN as the fully reduced one, the percentage of oxidized nucleotides was determined as (fully oxidized–control)/(fully oxidized–fully reduced). These calculations were done from data at Figure 5 at 520 nm (spectral maximum in control) and revealed that while in control conditions the cells were oxidized to about 56%, in photobleached cells, the number of oxidized nucleotides was decreased to 36% and thus by 20%. These data therefore point to functional effect of the photobleaching on the cardiomyocyte metabolism.

To evaluate the precise contribution of individual autofluorescence component responsiveness to metabolic modulators, we have applied linear unmixing algorithm on multispectral autofluorescence images of modulated cardiomyocytes (Fig. 6). In the absence of modulators, the rate of the photobleaching induced by scanning with 1–5 min recovery breaks (Fig. 6b, o) was slower for all three components. The fluorescence of component 2 and component 3, but not that of component 1, even spontaneously recovered.

In cells exposed to photobleaching (Fig. 6b, i), as well as those without photobleaching (Fig. 6b, ii), the fluorescence of component 1 was the most responsive to uncoupling, as its

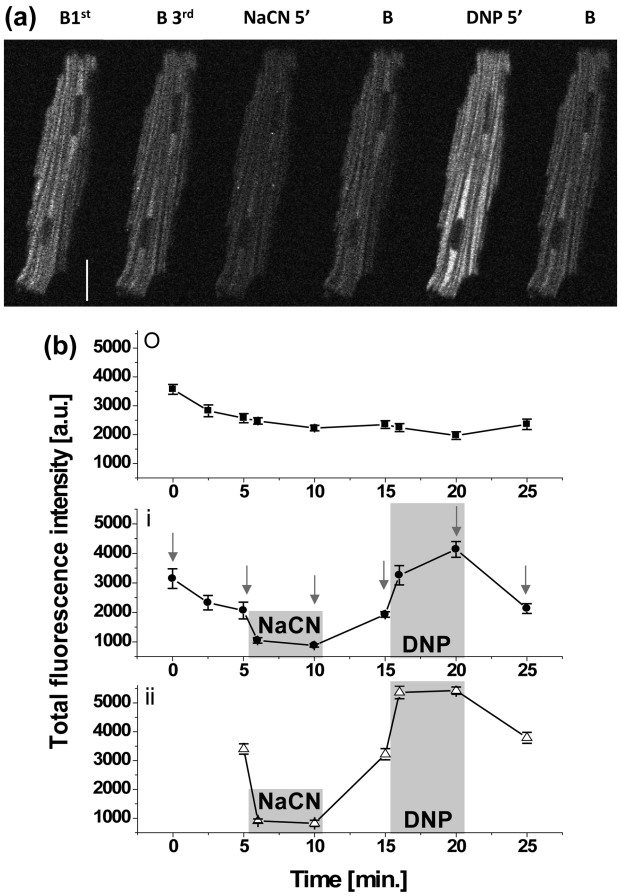

Figure 4. The effect of photobleaching on metabolic modulation of flavin autofluorescence. (**a**) Image of representative cardiomyocyte in control conditions and after the 1st scan (B1st) versus the 3rd consecutive scan (B3rd), and/or in the presence of 5 min metabolic modulation with 4 mmol/l of NaCN and/or 50 μmol/l of DNP; return to control (B). Scale bar: 20 μm. (**b**) Averaged autofluorescence emission spectra ± SEM (n = 7) of single cardiomyocytes without perfusion (o) obtained by successive scanning (-■-), and perfused with modulators of mitochondrial respiratory chain after photobleaching (i) obtained after third scan (-●-) or without photobleaching (ii) obtained after first scan (-Δ-).

fluorescence increased about two-fold. Also, altered cell functioning in cells exposed to multiple scanning was observed by slower, gradual responsiveness of all three autofluorescence components to mitochondrial modulators when compared to immediate autofluorescence changes in cells exposed to one scan only. The fluorescence of component 1 recovered neither spontaneously in control conditions, during the recovery intervals or after NaCN washout, nor when its increase was induced by application of DNP. Its fluorescence returned to the bleached level after DNP washout. These results clearly indicate the role of component 1 in functional repercussion of photobleaching on the cell behavior.

In the last step, taking into consideration our findings of the repercussions of photobleaching on the cell metabolic state, we aimed to evaluate whether this is also reflected on the cell contractility, one of the most important parameters characterizing cardiac cell functioning. Flavin fluorescence intensity (Fig. 7a,c) was recorded together with the cardiomyocyte contraction at 0.5 Hz (Fig. 7b,d). Our data demonstrated that significant decrease in the fluorescence intensity induced by photobleaching (Fig. 7c) led, in the same cells, to significant rise in the cell contractility (Fig. 7d), indicating functional repercussions of the induced photodamage. These experiments demonstrate that induced photobleaching had an impact on the functional outcome of the cardiac cell—the cardiomyocyte contractility.

Discussion

Experiments with multiple scanning of images with 458 nm laser line and detection of fluorescence in multispectral mode revealed an abrupt and spectrally heterogenous photobleaching of cellular flavin endogenous fluorescence in cardiomyocytes. Similar shapes of decay curves of total flavin autofluorescence due to photobleaching were also observed in cardiomyocytes using 350–480 nm band pass lamp, 488 nm laser (20), and 900 nm two-photon excitation (21).

Photobleaching is a dynamic process in which fluorochrome molecules undergo photoinduced chemical destruction upon exposure to excitation light and thus lose their ability to emit fluorescence (28). Recording of the flavin fluorescence by spectral-resolved microscopy showed that photobleaching induced by consecutive scanning is dependent on the radiant exposure of the sample, rather than on the laser power (29). This result is in agreement with previous observations (13), where various levels of radiant exposure induced the photobleaching of cardiomyocyte flavin autofluorescence comparable to our results.

Flavins are known to be rather photolabile (30). Their isoalloxazine chromophores system also constitutes the redox active moiety of the flavin coenzymes. One of the photochemical degradation pathways for riboflavin compounds is the intramolecular photoreduction involving ribityl side chain dehydrogenation and reduction in the isoalloxazine nucleus. It results in the formation of products more susceptible to photolysis and hydrolysis (30). Photoreduction of flavins, a photochemical reaction that leads to a loss of fluorescence as the quantum yield of reduced flavin, is very low, and reduced flavin does not absorb light at blue-light excitation (30).

In in vitro conditions, at low excitation intensities, flavin photoreduction is reversible and oxygenation of rapidly photoreduced flavin solutions results in spectra essentially identical to those obtained before light exposure and thereby indicates that no significant photodecomposition of the flavins occurs (15). At higher excitation intensities, however, the system builds up a population of nonfluorescent molecules due to subsequent photobleaching and photodestruction (30).

In living cells, illumination by bright light causes the decrease in flavin autofluorescence. We observed that altered fluorescence was accompanied by change in the fluorescence spectra with shifted emission maximum and lower intensity.

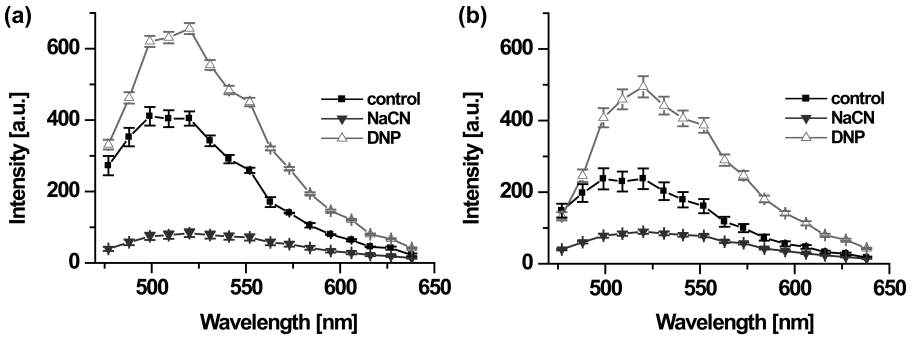

Figure 5. The effect of photobleaching on flavin autofluorescence spectra during metabolic modulation. (**a**) Averaged flavin fluorescence emission spectra ± SEM (λ_{exc} 458 nm/λ_{em} 477–638 nm) of single cardiomyocytes perfused with modulators of mitochondrial respiratory chain obtained by scanning of different cells (n = 7) after the first scan (in the absence of photobleaching), versus (**b**) after the third scan (after photobleaching). Emission spectra measured in basic external solution (-●-), after 5 min perfusion with 4 mmol/l NaCN (-▼-), and after 5 min perfusion with 50 μmol/l DNP (-Δ-).

This suggests that, besides photoreduction, part of the flavin pool was also photodestructed. Application of linear unmixing algorithm on spectrally resolved images allowed us to investigate photobleaching of individual components separately. These results revealed that spectrally heterogeneous decrease in autofluorescence emission due to photobleaching is caused by different bleaching rates of individual flavin components. The highest bleaching rate of component 1, ascribed to flavoproteins ETF and LipDH (8), could be explained by the fact that, in flavoproteins, photochemical destruction in flavoenzymes is accompanied with concomitant release of the flavin cofactor (30). Also, flavin cofactor is bound to the protein in an extended conformation. The intramolecular quenching of the FAD molecule in flavoproteins is therefore removed (30), and flavin bound in LipDH has considerably higher fluorescence quantum yield ~0.1 when compared to free FAD ~0.03 (30). We therefore consider that abrupt fall in fluorescence of component 1 might be due to photodestruction accompanied by release of FAD cofactor after exposure to high excitation intensity. Slower rate of photobleaching of components 2 and 3 ascribed to free FAD and to acyl-coA dehydrogenase, respectively (8), and partial recovery of fluorescence of during recovery intervals suggest that other mechanisms of photobleaching and inherent recovery are also involved.

Although passive diffusion or active translational processes of unbleached molecules into the observed area are proposed in various studies to be responsible for recovery of fluorescence after photobleaching, we do not expect this mechanism to be involved in our study, because the sources of flavin fluorescence are localized in mitochondria and are not likely to diffuse. Moreover, the whole volume of the cell was exposed to bleaching, since the whole area was scanned, and in single photon microscopy, the whole specimen is exposed to high intensity excitation light.

We also tested whether the photobleaching affected the responsiveness of the cell to metabolic modulators. In cells unexposed to previous scanning, fluorescence changes of all three components induced by application of mitochondrial modulators NaCN and DNP were fully reversible after the washout of both of modulators. Decrease in fluorescence after application of NaCN being due to block of the Complex IV of the respiratory chain (11), the recovery of fluorescence after NaCN washout is thus due to reoxidation of flavins after NaCN block removal. In contrast, as the increase in the fluorescence after application of DNP is due to uncoupling, we propose that the decrease of fluorescence after DNP washout is due to the reduction of flavins after removal of the protonophore.

In cells exposed to previous scanning, however, altered and delayed responsiveness to metabolic modulators was observed. Gathered data shows that percentage of oxidized nucleotides was decreased of about 20% of its original value, indicating that the cells are in a more reduced state. Decrease in fluorescence of component 1 was observed in control conditions prior to metabolic modulation. Only part of component 1 pool seemed to be involved in responses to mitochondrial modulators, smaller in amplitude when compared to unimpaired cells. This result suggests that this part of component 1 pool was irreversibly photo-destructed. In contrast, fluorescence of component 2 and component 3 returned to the initial level after DNP washout. We propose that such reversible decrease in the fluorescence of these components after multiple scanning was due to photoreduction, and return of fluorescence for these components was accomplished by their reoxidation in the respiratory chain either spontaneously during the recovery intervals, or induced by DNP.

In cardiomyocytes, enzyme-dependent fluorescence recovery after photobleaching of coenzymes involved in redox reactions was described for NADH (31). Return of bleached NADH (which is fluorescent in reduced form) is proposed via reduction of NAD^+ pool by reductases. NADH signal returns to the original steady state level, suggesting that the photodamage to the NADH generation system is minimal (31). Our previous work on photobleaching of time-resolved spectra of NADH fluorescence in cardiomyocytes (22) revealed only limited damage, but the study was

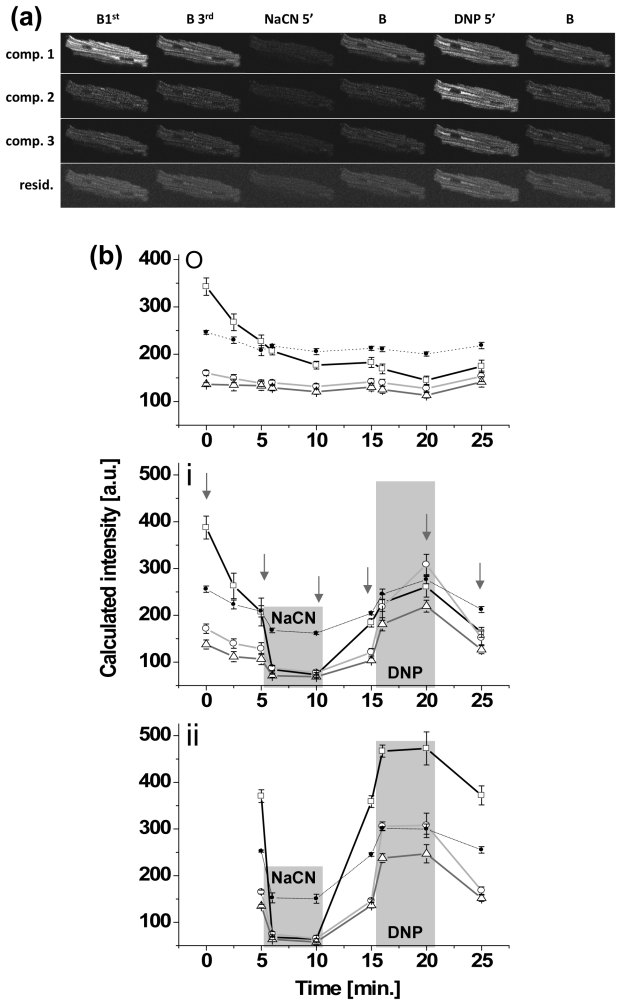

Figure 6. The effect of metabolic modulation on unmixed individual flavin autofluorescence components during photobleaching. (**a**) Representative image of cardiomyocyte flavin fluorescence resolved after linear unmixing of its spectral components is shown after the 1st scan ($B1^{st}$) versus the 3rd consecutive scan ($B3^{rd}$) and/or in the presence of 5 min metabolic modulation with 4 mmol/l of NaCN and/or 50 μmol/l of DNP; return to control (B). (**b**) Comparison of the change in the fluorescence intensity of individual spectral fluorescence component 1 (-□-), component 2 (-●-), component 3 (○), and its residues (Δ) with six consecutive scans computed by principal component analysis. Averaged autofluorescence emission intensity ± SEM (n = 7) is shown in control conditions without modulators (o) and with modulators in the presence of photobleaching after the third scan (i), or in the absence of photobleaching after the first scan (ii).

not done by imaging. In the present case, however, we observed altered autofluorescence responses to mitochondrial modulators in bleached cells. Namely, the responsiveness to DNP was lowered, suggesting that the bleached cells are in a more reduced state. This result indicates that besides photoreduction, also photodestruction is observed. This is in agreement with early observations of inactivation of mitochondrial enzymes after live cell exposure to visible light (32). Besides inactivation, violet-blue light is also suggested to stimulate H_2O_2 production in peroxisomes and mitochondria via activation of flavin-containing oxidases (33).

Flavin fluorescence photobleaching was associated, in recorded cells, with significant changes in the cardiomyocyte contractility. This observation is in agreement with the fact that main effect was observed at the level of the component I (ETF/LipDH), so at the level of mitochondrial respiratory chain. These results also correspond to cells being in a reduced state after photobleaching. This clearly points to functional repercussions of the effect of photobleachinng on the cell metabolism. When compared to other observations of photodamage in living cells using fluorescence microscopy, cell photodamage due to flavin photobleaching was in our study more emergent and intense. Namely, the lack of an immediate photobleaching decay of NADH cellular autofluorescence with the first acquired frame is observed at low excitation intensities (34). A defined laser-power threshold inducing photodamage was related to sudden drop or rise of fluorescence of Ca^{2+}-sensitive indicators (35,36). Observed effect on contractility thus may be ascribed to modification of calcium kinetics. Experiments with attenuated laser-power showed considerable photobleaching even at low excitation power and decrease of fluorescence was non-negligible for the whole range of excitation conditions (already after the first scan). Also, within the applied range of radiant exposure values we observed substantial flavin photobleaching, yet no other apparent signs of damage to cardiomyocytes, such as formation of bright circular lesions (34) or blurred z-lines, spontaneous contractions and blebbing (31), were observed. Photobleaching of naturally occurring fluorophores is therefore important to take into consideration also in other types of patho-/physiological and metabolism experiments, where low laser excitation powers are used and no other apparent signs of photodamage are observed. Consequently, photobleaching has to be assessed in all situations, where functional measurements are taken and conclusions on the cell state driven.

Overall data gathered in this work revealed that successive scanning of the same cell in the multispectral mode caused deviations in the shape of fluorescence emission spectrum due to inhibition of the respiratory chain and putting cells in a more reduced state. Consequently, such approach is not suitable for determination of fine changes in spectral shape reflecting redox state of flavins and flavoproteins altered by modulators. Instead, we propose performing such measurements each time on a different cell and then to compare averaged emission spectra between populations. Spectra obtained from successive scans should be used with great care and deterioration of signal by photobleaching always has to be taken into consideration. Considerable photobleaching, which causes alterations in responsiveness to mitochondrial modulators, was also observed in experiments where attenuated laser powers were used. Therefore, the possibility that energy metabolism is altered needs to be considered in all experiments where the light excitation induces flavin absorption.

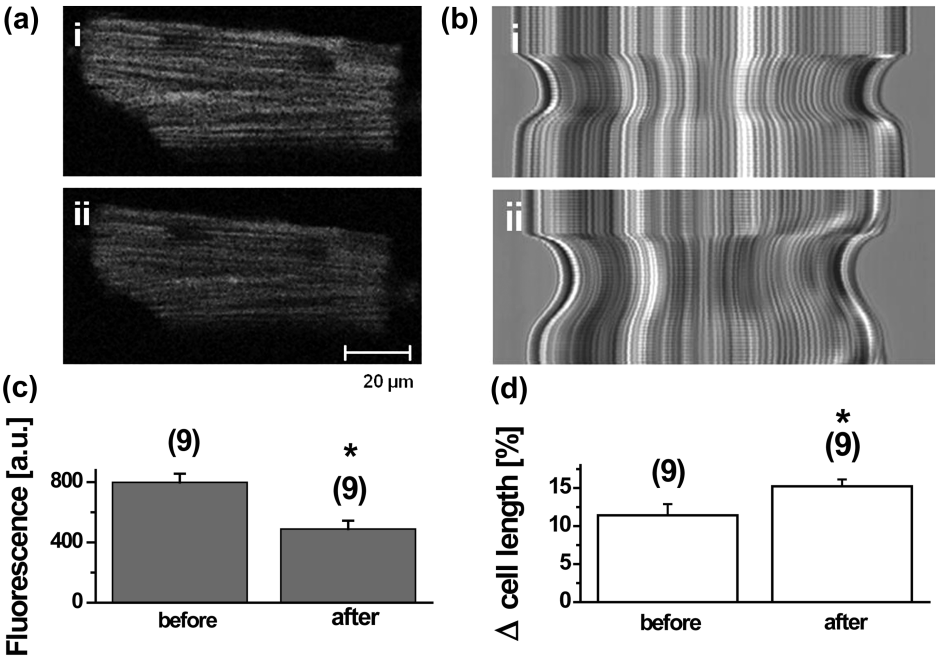

Figure 7. The effect of photobleaching on cardiomyocyte contractility. (**a**) Cardiomyocyte flavin fluorescence image (λ_{exc} 458 nm/λ_{em} 477–638 nm) before and after extensive bleaching of cardiomyocyte autofluorescence by 488 nm Ar:ion laser line at room temperature in control (i) and after bleaching (ii). (**b**) Example of contractility measurement by transmission line-scanning mode. Picture demonstrates maximal cell length at relaxed state and minimal cell length at contraction state induced by field stimulation at 0.5 Hz at room temperature in control (i) and after bleaching (ii). (**c**) Cardiomyocyte flavin fluorescence intensity, expressed as average ± SEM (n = 9), before and after bleaching. (**d**) Cardiomyocyte shortening induced by field stimulation at 0.5 Hz, expressed as percentage of maximal cell length at relaxed state at room temperature before and after bleaching. Data are expressed as average ± SEM (n = 9).

Conclusions

In the present study, we have analyzed in details photobleaching of endogenous flavins fluorescence in living cardiac cells in the course of spectrally-resolved confocal imaging. We demonstrated nonuniform photobleaching due to different photobleaching rates of individual flavin components, leading to photodamage which caused significant alterations in normal cell functioning, as monitored by responsiveness to metabolic modulators and by cell contraction, but without obvious changes in the cell morphology. These findings need to be taken in account when metabolic screening is performed, as well as in both qualitative and quantitative studies using endogenous flavin fluorescence and thus in all studies involving visible light excitation and fluorescence acquisition in living cells.

Acknowledgments

This publication was supported by SASPRO grant no 0063/01/02 financed by the Slovak Academy of Sciences and by a "Co-financing of regional, national and international programs (COFUND)", which is part of the Marie Curie Action of the EU 7th Framework Programme, under grant agreement no 609427, as well as the VEGA Grant Agency under contract nos 2/0169/16 and 2/0123/18. Authors also acknowledge support from the Integrated Initiative of European Laser Infrastructures LASERLAB-EUROPE IV (H2020 grant agreement no 654148).

Conflict of Interest

None declared.

Literature Cited

1. Chorvatova A, Chorvat D, Jr. Review of tissue fluorophores and their spectroscopic characteristics. In: Marcu L, French P, Elson D, editors. Fluorescence Lifetime Spectroscopy and Imaging for Tissue Biomedical Diagnostics. 1st ed. Boca Raton, FL: CRC Press; 2014. pp 1–15.
2. Kumar S, Dunsby C, De Beule PA, Owen DM, Anand U, Lanigan PM, Benninger RK, Davis DM, Neil MA, Anand P, et al. Multifocal multiphoton excitation and time correlated single photon counting detection for 3-D fluorescence lifetime imaging. Opt Express. 2007;15(20):12548–12561.
3. Rodrigues RM, Macko P, Palosaari T, Whelan MP. Autofluorescence microscopy: A non-destructive tool to monitor mitochondrial toxicity. Toxicol Lett. 2011;206(3): 281–288.
4. Rosner J, Liotta A, Angamo EA, Spies C, Heinemann U, Kovacs R. Minimizing photodecomposition of flavin adenine dinucleotide fluorescence by the use of pulsed LEDs. J Microsc. 2016;264(2):215–223.
5. Konig K, Becker TW, Fischer P, Riemann I, Halbhuber KJ. Pulse-length dependence of cellular response to intense near-infrared laser pulses in multiphoton microscopes. Bioessays. 1999;39(8):1700003.
6. Icha J, Weber M, Waters JC, Norden C. Phototoxicity in live fluorescence microscopy, and how to avoid it. Bioessays. 2017;39(8):1700003.
7. Chorvat D Jr, Bassien-Capsa V, Cagalinec M, Kirchnerova J, Mateasik A, Comte B, Chorvatova A. Mitochondrial autofluorescence induced by visible light in single rat cardiac myocytes studied by spectrally resolved confocal microscopy. Laser Phys. 2004;14(2):220–230.
8. Chorvat D Jr, Kirchnerova J, Cagalinec M, Smolka J, Mateasik A, Chorvatova A. Spectral unmixing of flavin autofluorescence components in cardiac myocytes. Biophys J. 2005;89(6):L55–L57.
9. Romashko DN, Marban E, O'Rourke B. Subcellular metabolic transients and mitochondrial redox waves in heart cells. Proc Natl Acad Sci U S A. 1998;95(4): 1618–1623.

10. Scholz R, Thurman RG, Williamson JR, Chance B, Bucher T. Flavin and pyridine nucleotide oxidation-reduction changes in perfused rat liver. I. Anoxia and subcellular localization of fluorescent flavoproteins. J Biol Chem. 1969;244(9):2317–2324.
11. Chance B, Ernster L, Garland PB, Lee CP, Light PA, Ohnishi T, Ragan CI, Wong D. Flavoproteins of the mitochondrial respiratory chain. Proc Natl Acad Sci U S A. 1967;57(5):1498–1505.
12. Kunz WS, Kunz W. Contribution of different enzymes to flavoprotein fluorescence of isolated rat liver mitochondria. Biochim Biophys Acta. 1985;841(3):237–246.
13. Koke JR, Wylie W, Wills M. Sensitivity of flavoprotein fluorescence to oxidative state in single isolated heart cells. Cytobios. 1981;32(127–128):139–145.
14. Skala MC, Riching KM, Gendron-Fitzpatrick A, Eickhoff J, Eliceiri KW, White JG, Ramanujam N. In vivo multiphoton microscopy of NADH and FAD redox states, fluorescence lifetimes, and cellular morphology in precancerous epithelia. Proc Natl Acad Sci U S A. 2007;104(49):19494–19499.
15. McCormick DB, Koster JF, Veeger C. On the mechanisms of photochemical reductions of FAD and FAD-dependent flavoproteins. Eur J Biochem. 1967;2(4):387–391.
16. Kindzelskii A, Petty HR. Fluorescence spectroscopic detection of mitochondrial flavoprotein redox oscillations and transient reduction of the NADPH oxidase-associated flavoprotein in leukocytes. Eur Biophys J. 2004;33(4):291–299.
17. Kunz WS. Spectral properties of fluorescent flavoproteins of isolated rat liver mitochondria. FEBS Lett. 1986;195(1–2):92–96.
18. Kunz WS, Gellerich FN. Quantification of the content of fluorescent flavoproteins in mitochondria from liver, kidney cortex, skeletal muscle, and brain. Biochem Med Metab Biol. 1993;50(1):103–110.
19. Kunz WS, Winkler K, Kuznetsov AV, Lins H, Kirches E, Wallesch CW. Detection of mitochondrial defects by laser fluorimetry. Mol Cell Biochem. 1997;174(1–2):97–100.
20. Rocheleau JV, Head WS, Piston DW. Quantitative NAD(P)H/flavoprotein autofluorescence imaging reveals metabolic mechanisms of pancreatic islet pyruvate response. J Biol Chem. 2004 July 23;279(30):31780–31787.
21. Huang S, Heikal AA, Webb WW. Two-photon fluorescence spectroscopy and microscopy of NAD(P)H and flavoprotein. Biophys J. 2002;82(5):2811–2825.
22. Chorvatova A, Mateasik A, Chorvat D. Laser-induced photobleaching of NAD(P)H fluorescence components in cardiac cells resolved by linear unmixing of TCSPC signals. In: Proceedings of SPIE—The International Society for Optical Engineering, Bellingham; 2011.
23. Bassien-Capsa V, Fouron JC, Comte B, Chorvatova A. Structural, functional and metabolic remodeling of rat left ventricular myocytes in normal and in sodium-supplemented pregnancy. Cardiovasc Res. 2006;69(2):423–431.
24. Chorvatova A, Hussain M. Effects of caffeine on potassium currents in isolated rat ventricular myocytes. Pflugers Arch. 2003;446(4):422–428.
25. Dickinson ME, Bearman G, Tilie S, Lansford R, Fraser SE. Multi-spectral imaging and linear unmixing add a whole new dimension to laser scanning fluorescence microscopy. Biotechniques. 2001;31(6):1272–1276.
26. Chorvatova A, Mateasik A, Chorvat D Jr. Spectral decomposition of NAD(P)H fluorescence components recorded by multi-wavelength fluorescence lifetime spectroscopy in living cardiac cells. Laser Phys Lett. 2013;10(12):125703.
27. Chorvatova A, Aneba S, Mateasik A, Chorvat D, Comte B. Time-resolved fluorescence spectroscopy investigation of the effect of 4-hydroxynonenal on endogenous NAD(P)H in living cardiac myocytes. J Biomed Opt. 2013;18(6):67009.
28. Song L, Hennink EJ, Young IT, Tanke HJ. Photobleaching kinetics of fluorescein in quantitative fluorescence microscopy. Biophys J. 1995 June;68(6):2588–2600.
29. Schwille P, Haupts U, Maiti S, Webb WW. Molecular dynamics in living cells observed by fluorescence correlation spectroscopy with one- and two-photon excitation. Biophys J. 1999;77(4):2251–2265.
30. van den Berg PA, Widengren J, Hink MA, Rigler R, Visser AJ. Fluorescence correlation spectroscopy of flavins and flavoenzymes: Photochemical and photophysical aspects. Spectrochim Acta A: Mol Biomol Spectrosc. 2001;57(11):2135–2144.
31. Combs CA, Balaban RS. Direct imaging of dehydrogenase activity within living cells using enzyme-dependent fluorescence recovery after photobleaching (ED-FRAP). Biophys J. 2001;80(4):2018–2028.
32. Cheng LY, Packer L. Photodamage to hepatocytes by visible light. FEBS Lett. 1979;97(1):124–128.
33. Hockberger PE, Skimina TA, Centonze VE, Lavin C, Chu S, Dadras S, Reddy JK, White JG. Activation of flavin-containing oxidases underlies light-induced production of H_2O_2 in mammalian cells. Proc Natl Acad Sci U S A. 1999;96(11):6255–6260.
34. Tiede LM, Nichols MG. Photobleaching of reduced nicotinamide adenine dinucleotide and the development of highly fluorescent lesions in rat basophilic leukemia cells during multiphoton microscopy. Photochem Photobiol. 2006 May;82(3):656–664.
35. Hopt A, Neher E. Highly nonlinear photodamage in two-photon fluorescence microscopy. Biophys J. 2001;80(4):2029–2036.
36. Koester HJ, Baur D, Uhl R, Hell SW. Ca^{2+} fluorescence imaging with pico- and femtosecond two-photon excitation: Signal and photodamage. Biophys J. 1999;77(4):2226–2236.